HHS Public Access

Author manuscript

Sci Transl Med. Author manuscript; available in PMC 2021 August 20.

Published in final edited form as:

Sci Transl Med. 2018 May 23; 10(442): . doi:10.1126/scitranslmed.aal2563.

Adult rat myelin enhances axonal outgrowth from neural stem cells

Gunnar H. D. Poplawski[1,*,†], **Richard Lie**[1,†], **Matt Hunt**[1], **Hiromi Kumamaru**[1], **Riki Kawaguchi**[2], **Paul Lu**[1,3], **Michael K. E. Schäfer**[4], **Grace Woodruff**[5], **Jacob Robinson**[1], **Philip Canete**[1], **Jennifer N. Dulin**[1], **Cedric G. Geoffroy**[1], **Lutz Menzel**[4], **Binhai Zheng**[1], **Giovanni Coppola**[2], **Mark H. Tuszynski**[1,3,‡]

[1]Department of Neurosciences, University of California, San Diego, La Jolla, CA 92093, USA.

[2]Departments of Psychiatry and Neurology, University of California, Los Angeles, Los Angeles, CA 90095, USA.

[3]Veterans Administration Medical Center, San Diego, CA 92161, USA.

[4]Department of Anesthesiology and Focus Program Translational Neurosciences, Medical Center of the Johannes Gutenberg-University, Mainz, Germany.

[5]Department of Cellular and Molecular Medicine, University of California, San Diego, La Jolla, CA 92093, USA.

Abstract

Axon regeneration after spinal cord injury (SCI) is attenuated by growth inhibitory molecules associated with myelin. We report that rat myelin stimulated the growth of axons emerging from rat neural progenitor cells (NPCs) transplanted into sites of SCI in adult rat recipients. When plated on a myelin substrate, neurite outgrowth from rat NPCs and from human induced pluripotent stem cell (iPSC)–derived neural stem cells (NSCs) was enhanced threefold. In vivo, rat NPCs and human iPSC–derived NSCs extended greater numbers of axons through adult central nervous system white matter than through gray matter and preferentially associated with rat host myelin. Mechanistic investigations excluded Nogo receptor signaling as a mediator of

‡Corresponding author. mtuszynski@ucsd.edu.
*Present address: Department of Medicine, National University of Singapore, Singapore, Republic of Singapore.
†These authors contributed equally to this work.

Author contributions: G.H.D.P., R.L., M.H., and M.H.T. conceptualized the study. G.H.D.P., R.L., R.K., G.C., and M.H.T. performed analysis of transcriptomic data. G.H.D.P., R.L., M.H., R.K., G.C., H.K., and L.M. performed data validation. P.L. performed experiments for Figs. 1A and 2A; J.R. performed experiments for Fig. 1 (B and C); M.H. performed experiments and analysis for Fig. 2 (B to F); R.L. performed experiments and analysis for Figs. 3 to 5 (A to E), 6, and 7 (A, C, and D) and figs. S1, S2, and S5; G.H.D.P. performed experiments and analysis for Figs. 3 (K to N), 5 (F and G), 6, and 7 (E and F) and figs. S1 to S5 and S8; G.W. performed experiments for Fig. 3 (K to N); H.K. performed experiments and analysis for Fig. 7B and fig. S7A; R.K. and H.K. performed analysis for figs. S6 and S7B; L.M. performed experiments and analysis for Fig. 5 (A to C); J.N.D. performed experiments for Fig. 4 (C and D); C.G.G. performed experiments for Fig. 5E; and P.C. performed experiments and analysis for Fig. 7 (E and F). M.K.E.S., G.W., C.G.G., B.Z., G.C., and M.H.T. provided materials used for the experiments. R.K. and G.C. performed data curation. G.H.D.P., R.L., and M.H.T. wrote the original draft; G.P., R.L., M.H., P.L., R.K., M.H.T., C.G.G., B.Z., and G.C. reviewed and edited the manuscript.

Competing interests: The authors declare that they have no competing interests.

SUPPLEMENTARY MATERIALS

www.sciencetranslationalmedicine.org/cgi/content/full/10/442/eaal2563/DC1

stem cell–derived axon growth in response to myelin. Transcriptomic screens of rodent NPCs identified the cell adhesion molecule neuronal growth regulator 1 (Negr1) as one mediator of permissive axon-myelin interactions. The stimulatory effect of myelin-associated proteins on rodent NPCs was developmentally regulated and involved direct activation of the extracellular signal–regulated kinase (ERK). The stimulatory effects of myelin on NPC/NSC axon outgrowth should be investigated further and could potentially be exploited for neural repair after SCI.

INTRODUCTION

Regenerative growth of axons in the injured central nervous system (CNS) is strongly inhibited by molecules associated with adult myelin, including Nogo (1–4), myelin-associated glycoprotein (MAG) (5, 6), oligodendrocyte myelin glycoprotein (OMgp) (7, 8), netrin (9), ephrins (10), and other molecules (4). Experimental efforts in the field of CNS regeneration research have sought to target myelin-associated inhibitors, with resultant increases in adult axonal growth (2, 11, 12). Typically, measures to neutralize myelin-associated inhibitors generate growth of up to several hundred axons in the host spinal cord over distances of up to a few millimeters (2, 11, 12).

Recently, we reported that grafts of rodent neural progenitor cells (NPCs) or human neural stem cells (NSCs) into adult spinal cord lesion sites in rodent models resulted in the outgrowth of tens of thousands of stem cell–derived axons over distances as long as 50 mm through adult spinal cord white matter (13–16). Such growth is consistently observed with stem cells from mouse, rat, and human sources (13–15). The number and distance over which stem cells extend axons from spinal cord lesion sites collectively exceed that of adult axons by 1000- to 10,000-fold (17). Notably, NPCs and NSCs normally extend their axons during CNS embryonic development, well before extensive myelination has occurred. These observations prompted us to investigate interactions between adult CNS myelin and immature axons that extend from stem cell grafts placed in lesion sites of rats with spinal cord injury (SCI). A previous study reported that postnatal day 4 cerebellar granule neurons cultured on a single myelin protein component MAG showed less inhibition of neurite outgrowth than did adult neurons plated on the same substrate (6). Another study reported that embryonic day (E) 17 mouse spinal cord neurons exhibited increased neurite outgrowth on a MAG or myelin-oligodendrocyte glycoprotein (MOG) substrate compared to a control substrate (18). However, neurite outgrowth from rat E14 to E15 retinal ganglion cell neurons was inhibited by myelin (19). Previous studies have not examined neurite outgrowth from developing spinal cord neurons on whole myelin extracts, which collectively contain at least six proteins that inhibit neurite outgrowth (1–10).

Here, we examined whether whole myelin extracts inhibited neurite outgrowth from rodent developing neurons as a function of developmental stage and whether axonal outgrowth in vivo was influenced by myelin. We report that axons from rodent NPCs and from human iPSC–derived NSCs were not inhibited or repelled, but rather were stimulated, by adult rat CNS myelin.

RESULTS

NPC-derived axons preferentially extend through adult host white matter in vivo

We grafted rat E14–derived, green fluorescent protein (GFP)–expressing multipotent NPCs to sites of a C5 right hemisection spinal cord lesion in four adult F344 rats and compared axonal outgrowth in recipient rat host white matter versus gray matter after 2 weeks (Fig. 1). Tens of thousands of axons emerged from the lesion/graft site as previously reported (14, 15), extending over long distances through white matter (Fig. 1A). Quantification of NPC-derived axonal numbers in transverse sections at C8, four spinal cord segments below the lesion/graft site, revealed a significant, fourfold greater number of axons in white matter compared to gray matter, which contains little myelin ($P < 0.05$, paired t test; Fig.1, B to D).

NPC-derived axons preferentially associate with host myelin in vivo

To determine whether NPC-derived axons exhibited preferential association with myelin membranes in vivo when growing caudal to an SCI lesion site, we performed immunohistochemical and electron microscopic analysis of graft-derived axons associated with host myelin in vivo. Rat E14–derived multipotent NPCs were grafted to sites of C5 right hemisection injury, and 3 months later, we quantified the proportion of GFP-labeled axons per field that contacted myelin membranes (Fig. 2). Sixty-five percent of GFP-labeled, graft-derived axons contacted a myelin membrane per field examined, which was significantly greater ($P < 0.05$, Z test) than predicted if axons randomly extended through the same fields (40%; Fig. 2F). To investigate whether axons derived from human NSCs also associated with rat host myelin, we grafted NSCs derived from human iPSCs into sites of a C5 right hemisection lesion in rats. Three months later, graft-derived human axons were observed to be closely associated with MBP-immunoreactive rat host myelin. This interaction was assessed six spinal segments caudal to the lesion/graft site (Fig. 2A). Graft-derived human axons were associated with both intact host myelin sheaths (in ascending systems) and degenerating myelin (in descending systems) (Fig. 2, B to E).

NPC axon growth is stimulated by a CNS myelin membrane substrate

To understand mechanisms underlying potential myelin-mediated effects on outgrowth of NPC-derived axons, we used in vitro models. First, we confirmed that neurite outgrowth from adult rat dorsal root ganglion (DRG) neurons was inhibited when the neurons were plated onto myelin isolated from adult rat spinal cord (Fig. 3, A to D and I) (11, 20). Adult rat DRG neurons were dissociated and plated on the following substrates: PDL, laminin, myelin, or laminin plus myelin for 48 hours, and neurite extensions were assessed in neurons using anti–βIII-tubulin antibody. As expected from previous work (11, 20), neurite outgrowth from adult DRG neurons was increased threefold when plated on laminin, and this effect was significantly attenuated by myelin [$P < 0.0001$, one-way analysis of variance (ANOVA), with $P < 0.0001$ post hoc Tukey's test, comparing a laminin/myelin substrate to laminin alone and a myelin substrate to laminin or laminin/myelin; Fig. 3, A to D and I]. In contrast, cultures of rat E14 spinal cord–derived multipotent NPCs exhibited growth activation when plated on myelin that exceeded the effects of plating on laminin alone (Fig. 3, E to H and J). Rat NPCs plated on laminin exhibited a significant, twofold increase in neurite outgrowth compared to a PDL substrate ($P < 0.0001$, one-way ANOVA; $P < 0.0001$

post hoc Tukey's test comparing laminin to PDL; Fig. 3J). Notably, when cultured on a myelin substrate, NPCs exhibited the greatest degree of neurite outgrowth (>3-fold increase compared to PDL, $P < 0.0001$ post hoc Tukey's test), which exceeded the growth-promoting effects of laminin ($P < 0.0001$, post hoc Tukey's test; Fig. 3J). The effects of myelin plus laminin did not differ from that of myelin alone ($P = 0.2$; Fig. 3J). Non-neural membranes prepared from rat liver tissue showed a significantly reduced potential to promote neurite growth from rat NPCs compared to myelin membranes (1.3-fold compared to 3.1-fold, $P < 0.0001$ post hoc Tukey's test; fig. S1A). Other characteristics of in vitro neurite outgrowth, including longest neurite and neurite branching, were also stimulated by myelin (fig. S1, B to D). These findings indicate that myelin specifically promoted neurite outgrowth from rat E14 spinal cord–derived NPCs, exceeding the effects of laminin. We confirmed using Tau1 labeling that myelin exerted its growth-promoting effects on the axonal compartment of rat E14 spinal cord–derived NPCs (fig. S3).

Axon outgrowth from human iPSC–derived NSCs increases in response to myelin

Axonal extensions from human NSCs also readily occur through adult white matter in the rodent injured spinal cord (14, 15). To determine whether axonal outgrowth from human NSCs was stimulated by myelin, we plated neurons purified from human iPSC–derived NSCs on laminin plus myelin substrates using the same methods used for rodent NPCs (Fig. 3, K and M). Human iPSC–derived neurons exhibited a significant 2.5-fold increase in neurite extension on a rat myelin substrate (one-way ANOVA with $P < 0.0001$ post hoc Tukey's test; Fig. 3N) and a twofold increase when plated on a monkey myelin substrate ($P < 0.001$; Fig. 3N) compared to laminin alone.

NPCs are inhibited by chondroitin sulfate proteoglycans

To determine whether the growth state of NPCs was specifically enhanced by myelin rather than reflecting a generalized state of activated growth in NPCs, we cultured E14-derived rat spinal cord NPCs on chondroitin sulfate proteoglycan (CSPG) substrates that are well known to inhibit the growth of injured adult axons (21, 22). Neurite outgrowth from E14-derived rat spinal cord NPCs was significantly inhibited by CSPGs in a dose-dependent manner ($P < 0.0001$ one-way ANOVA, with $P < 0.001$ post hoc Tukey's test; Fig. 4, A and B).

Myelin-induced growth is developmentally regulated

To assess whether the growth-promoting effects of myelin on rat NPC–derived neurite growth were developmentally regulated, we measured neurite outgrowth from cultures of rat spinal cord–derived NPCs prepared from E14 through E19 rat spinal cord. These cell preparations were plated on either PDL or PDL plus myelin (Fig. 4, C and D). Notably, the ability of myelin to promote neurite outgrowth steadily declined from a peak at E14 and E15 to a complete loss of the effect by E19 ($P < 0.0001$, one-way ANOVA; $P < 0.001$, post hoc Tukey's test, showing significant loss of neurite stimulation by E17 compared to E14 and E15; Fig. 4D). In a separate experiment, we plated E14-derived multipotent rat NPCs on PDL, allowed them to mature for 6 days in vitro, and assessed the effects of replating them onto a myelin substrate (fig. S4). Neurite outgrowth from these cells, at the "equivalent" biological age of E20, was significantly inhibited by myelin ($P < 0.001$, t test), supporting

the notion that the developmental age of NPCs was important for growth stimulation by myelin.

Myelin extracts directly activate neuron-intrinsic growth programs

To determine whether myelin activates classic signaling pathways in NPCs related to enhanced neurite outgrowth (23–25), we added myelin extracts to the media of cultures of dissociated rat E14 spinal cord–derived NPCs and examined phosphorylation of *ERK*. Three and six hours after myelin treatment, *ERK* was significantly activated in rat NPCs as determined by both Western blot and enzyme-linked immunosorbent assay (ELISA) ($P < 0.05$, Student's *t* test; Fig. 5, A to C). This finding suggested that a ligand in the soluble myelin extract was binding to neuronal surface receptors, leading to downstream activation of neuronal growth programs. Application of the *ERK* inhibitor CAS1049738 or the upstream mitogen-activated protein kinase (MAPK)/ERK kinase 1 (MEK) inhibitor PD98059 partially blocked myelin-mediated stimulation of neurite outgrowth in E14 rat spinal cord–derived NPCs (by 22 and 14%, respectively; $P < 0.001$, ANOVA; $P < 0.01$, post hoc Tukey's test; fig. S5A). The partial effects of ERK/MEK inhibition indicated that other signaling pathways were also likely to be involved in myelin-mediated stimulation of neurite growth. To determine whether the ligand in the myelin extract was vulnerable to methods that denatured proteins, we heated the myelin extract to 95°C for 30 min and observed a significant attenuation of myelin-induced neurite outgrowth from E14 rat spinal cord–derived NPCs ($P < 0.0001$, one-way ANOVA; $P < 0.0001$, post hoc Tukey's test comparing denatured myelin to naïve myelin; Fig. 5D). Confirming the protein nature of the myelin ligand, addition of proteinase K entirely abolished myelin-mediated activation of neurite outgrowth ($P < 0.0001$; Fig. 5D).

Some proteins that are present in adult myelin, such as *MAG* and netrin, are known to elicit opposing effects on axonal growth, switching between promotion/attraction and inhibition/repulsion depending on the developmental stage, neuronal receptor composition, and intracellular signaling pathways that are activated (6, 26, 27). To assess whether classic myelin-associated inhibitors of adult axon growth contribute to activation of neurite outgrowth from E14 rat spinal cord–derived NPCs, we plated NPCs on myelin isolated from single gene or triple-knockout animals lacking *Nogo*, *MAG*, and *OMgp* (11). Elimination of these myelin-associated proteins did not affect neurite outgrowth from rat NPCs (Fig. 5E), suggesting that other molecules might be facilitating NPC outgrowth on myelin.

Myelin-mediated outgrowth stimulation does not depend on elevated cAMP

Previous work from Filbin and colleagues demonstrated that the growth-promoting effects of MAG on young neurons was dependent on high concentrations of endogenous adenosine 3′,5′-monophosphate (cAMP) (26) and that elevated cAMP in mature neurons reduced neurite inhibition on MAG or myelin substrates (28). We demonstrate that myelin-mediated growth stimulation of rat NPCs on myelin was not associated with increased cAMP and that myelin reduced cAMP concentrations in rat NPCs ($*P = 0.05$, $**P < 0.01$, Student's *t* test; Fig. 5F). This reduction in cAMP was concomitant with increases in ERK (Fig. 5, F and D). Furthermore, when cAMP was elevated by forskolin administration, neurite outgrowth

from rat NPCs was reduced on myelin substrates, whereas outgrowth on PDL or laminin was increased ($P < 0.05$, Student's t test; Fig. 5G).

RNA sequencing is used to identify candidate molecular mechanisms of myelin stimulation

To further identify molecular mechanisms associated with myelin-induced stimulation of neurite outgrowth from E14 rat spinal cord–derived NPCs, we turned to RNA sequencing (RNA-seq). For this study, we used mouse NPCs to take advantage of mouse molecular genetics for candidate validation. First, we confirmed that neurite outgrowth from E12 mouse spinal cord–derived multipotent NPCs was also stimulated by myelin substrates; we found similar results to rat NPCs (fig. S2).

We then performed RNA-seq on E12 mouse spinal cord–derived NPCs that were plated for 48 hours on substrates of PDL, laminin, laminin/myelin, or myelin alone (Fig. 6C and fig. S6). Compared to PDL substrate, using a 10% FDR threshold, 616 transcripts were differentially expressed on a myelin substrate, 529 on a laminin/myelin substrate, and 157 on a laminin substrate (Fig. 6A); about 90% of these transcripts were down-regulated under growth-promoting conditions (Fig. 6A), suggesting that mechanisms enabling growth on myelin could be related to suppression of growth inhibitors. A total of 471 transcripts specifically changed when mouse NPCs were grown on myelin substrates compared to laminin substrates (Fig. 6B). Annotation of myelin substrate–induced transcripts yielded predicted functions related to the growth state of the cell, including cancer-related genes (a high cellular growth state), neuronal survival, differentiation and outgrowth, and formation of cellular protrusions (Z scores > 2 for myelin versus PDL; Fig. 6E). Gene ontology enrichment analysis of all up-regulated genes in response to myelin stimulation indicated preferential involvement of transmembrane receptor functions (Fig. 6D).

Negr1 mediates neurite growth on a myelin substrate in rat NPCs

One of the top transcripts that was up-regulated on a myelin substrate in our RNA-seq data set was neuronal growth regulator 1 (*Negr1*) (one-way ANOVA, with $P < 0.01$ post hoc Tukey's test; Fig. 7A). This protein, also known as Neurotractin or Kilon, encodes a glycosylphosphatidylinositol (GPI)–anchored cell adhesion molecule that has been reported to function as a transneural growth-promoting factor in regenerative axon sprouting in the murine brain (29). On the basis of this activity, we chose to focus on this candidate to determine whether it was required for myelin-induced enhancement of neurite outgrowth in mouse NPCs. First, we confirmed that *Negr1* mRNA and protein were increased in E12 mouse spinal cord–derived NPC cultures after 48 hours in vitro (mRNA: $P < 0.05$, unpaired t test, Fig. 7B; protein: $P < 0.05$, unpaired t test, Fig. 7, C and D). To determine whether expression of *Negr1* correlated with developmentally regulated changes in myelin-mediated neurite outgrowth in mouse NPCs (Fig. 4D), we quantified *Negr1* mRNA expression via quantitative polymerase chain reaction (qPCR) in mouse NPCs derived from E12, E15, and E19 mouse embryos. Myelin-stimulated increases in *Negr1* mRNA in mouse NPCs diminished from E12 to E19 ($P < 0.05$, Student's t test; Fig. 7B), concomitant with the known decline in myelin-mediated neurite growth with age (Fig. 4D and fig. S4). Negr1 has been postulated to increase ERK phosphorylation via signaling through FGFR2 (30);

this RNA-seq data set also showed statistically significant increases in *FGFR2* mRNA after growth of mouse NPCs on myelin (fig. S5B). We then investigated whether *Negr1* protein expression was essential for myelin-mediated neurite outgrowth from mouse NPCs in culture. NPCs from *Negr1*-deficient mice (31) were cultured on PDL and a myelin substrate for 48 hours in vitro. *Negr1* knockout mice showed no significant effects on neurite outgrowth from E12 mouse spinal cord–derived NPCs cultured on PDL (Fig. 7E). In contrast, when cultured on a myelin substrate, mouse NPCs deficient in *Negr1* showed a significant 25% reduction in myelin-mediated neurite outgrowth compared to *Negr1*-positive littermate control NPCs ($P < 0.05$, Student's *t* test; Fig. 7F). To determine whether overexpression of Negr1 could overcome inhibitory effects of myelin on more mature neurons, we transfected Negr1-pcDNA3 into E14 rat spinal cord–derived NPCs, matured them for 6 days in culture (a time point at which they become inhibited by myelin; fig. S4) and then replated the cells on myelin (fig. S8). Overexpression of Negr1 significantly overcame myelin inhibition, increasing total neurite length per cell by 37% ($P < 0.0001$, Student's *t* test).

DISCUSSION

The growth inhibitory effects of myelin on axon regeneration by injured adult CNS neurons remain an obstacle to promoting functional spinal cord regeneration. Several experimental strategies to attenuate myelin inhibition have been investigated in rodents (2, 11, 12) and, in one case, in human patients with SCI (32). As previously reported (13, 33), host axons readily regenerate into the myelin-free milieu of a stem cell implant and form synapses with NPCs or NSCs, which in turn extend axons into the host spinal cord beyond the lesion site forming their own synapses with host neurons. We show here that myelin functionally enhanced the neuritic growth state of rodent NPCs and human NSCs, and did so through interacting protein partners expressed by rodent NPCs including *Negr1*. The mechanisms underlying enhancement of NPC/NSC axon growth on a myelin substrate are based on specific ligand-mediated interactions, as noted above, and are not merely a reflection of a baseline state of enhanced growth regardless of environment given that neurite outgrowth from rat NPCs was strongly inhibited by CSPGs. Notably, myelin is not present during early CNS development when axons are actively extending. Myelin is only formed after termination of axonal patterning and the establishment of mature projections, initiated around birth (34). Previous work has shown that developing (35–40) and even adult (41, 42) neurons transplanted into the CNS of rodents and nonhuman primates (16) can extend long axons. In the current study, we show that myelin stimulates axon outgrowth from rat NPCs, but axon growth is blocked by CSPGs. Despite the accumulation of CSPGs around SCI sites (21, 43–45), rat NPC–derived axons are able to extend into the host spinal cord. NPC grafts have been shown to reduce reactive astrocytosis around spinal cord lesion sites by 80% [Fig. 3 in (13)], thereby attenuating a potential source of CSPGs (46–50).

There are a number of limitations to the current study. RNA-seq identified *Negr1* as a candidate cell adhesion molecule mediating myelin-related activation of neurite outgrowth, and studies of NPCs derived from *Negr1* knockout mice confirmed this candidate. *Negr1* is a member of the IgLON family of GPI-anchored cell adhesion molecules—the limbic system–associated membrane protein/opioid-binding cell adhesion molecule/neurotrimin

subgroup of the immunoglobulin superfamily (51)—and has been reported to promote neurite outgrowth in vitro (29, 31, 51). Given that *Negr1*-deficient mouse NPCs exhibited a 25% reduction in neurite outgrowth on a myelin substrate, other candidates identified by RNA-seq should be investigated to probe contributions of other molecules to myelin-mediated growth. Eventually, complete elucidation of contributing molecular mechanisms to myelin-mediated enhancement of NPC axon growth may allow the rational design of strategies to enable adult axon growth through SCI lesion sites. A second limitation of this study is that the total myelin extract used in our work might be more representative of myelin debris that is exposed at the lesion site rather than intact or degenerating myelin found in the spinal cord white matter rostral and caudal to the lesion. However, we found that axons emerging from NPC/NCS grafts placed into rat SCI sites were associated with degenerating and intact myelin sheets. Further studies should investigate whether NPC/NSC graft–derived axons are preferentially associated with intact myelin versus degenerating myelin and thus prefer to grow along intact versus degenerating white matter tracts. Finally, it will be of interest to identify the molecules within adult CNS myelin extract that promote axon growth. Fractionation of the myelin extract and consecutive isolation of the signaling molecules that stimulate axon growth could lead to the design of therapeutic compounds that could be applied in combination with stem cell therapy to promote greater axon growth.

Here, we have shown that adult myelin, which is inhibitory for axonal regeneration by adult neurons, stimulates the growth of axons emerging from rodent NPC grafts and human iPSC–derived NSC grafts. This effect is mediated in part by *Negr1* signaling. Just as growth cones may interpret the same guidance cue as either attractive or repulsive during development (52), our study suggests that axons growing from early-stage NPCs can perceive otherwise inhibitory myelin as growth-promoting in the injured adult CNS. These findings identify an advantage of NPC-based approaches for promoting neural repair and raise the possibility of identifying new ways to overcome the inhibitory effects of myelin on adult axon regeneration.

MATERIALS AND METHODS

Study design

We examined the effect of myelin on the outgrowth of axons from rodent NPCs both in vitro and in vivo. We performed in vitro assays of neurite outgrowth on a myelin substrate together with molecular analyses using minimal replicates of three for each experimental condition. For in vivo studies in rat, given large differences in neurite outgrowth in white versus gray matter, we used sample sizes between four and eight to test significant differences. Numbers of replicates are listed in each figure legend. All experiments were randomized with regard to animal enrollment into treatment group, and experimenters were blinded to experimental condition when performing data analyses.

Animals

A total of 38 rats were used, including 8 adult female Fischer 344 rats for grafting and 23 pregnant dams (3 GFP-positive) for embryonic tissue harvesting, and 7 athymic nude rats (The Jackson Laboratory) for grafting of human NSCs. A total of 18 pregnant mice

were used in this study for harvesting of embryonic tissue, including 12 C57BL/6 and 6 *Negr1*-deficient C57Bl/6 (31). The National Institutes of Health (NIH) guidelines for laboratory animal care and safety were strictly followed. Animals had free access to food and water throughout the study. All surgeries were performed under deep anesthesia using a combination (2 ml/kg) of ketamine (25 mg/ml), xylazine (1.3 g/ml), and acepromazine (0.25 mg/ml).

Transplantation surgeries and histology

Hemisection: Adult female Fischer 344 rats ($n = 8$) or athymic nude rats ($n = 7$) underwent C5 spinal cord lateral hemisection lesions, as described (14). Four rats were perfused 2 weeks after grafting to assess axon density in white versus gray matter in transverse sections at C8. Four rats were perfused 3 months after grafting and processed for electron microscopy (EM) (53). Human iPSC–derived NSCs were generated as described (15) and grafted (100,000 cells/μl) into C5 hemisection lesion sites of athymic nude rats, 2 weeks later. Survival time was 3 months. Animal perfusion, histology, and immunohistochemical staining was performed as described (14, 15).

EM studies

Rats ($n = 4$) with C5 lateral hemisection and 2-week-delayed GFP-expressing E14 NPC grafts were perfused 3 months after grafting, and tissue was processed for EM as described (53).

Membrane fractionation

Myelin extraction from fresh adult C57BL/6 mice, Fischer 344 rats, and frozen adult *Macaca mulatta* spinal cords was performed using sucrose-gradient centrifugation, as described (54). Total protein concentration of myelin was assessed using a Bradford protein assay (Bio-Rad). Myelin from transgenic mice was obtained from the Zheng laboratory (11).

Myelin denaturation

To denature protein components, myelin extracts were either incubated at 95°C for 30 min or treated with proteinase K at 37°C for 30 min before coating tissue culture plates.

Primary cell culture

DRG culture from adult C57BL/6 mice was prepared as previously described (55) and cultured in 48-well plates with 250 neurons per well. NPCs of E12 spinal cords from C57BL/6 mice or E14 to E19 Fischer 344 rats were prepared as described (13) and plated in 48-well plates at 10,000 cells/250 μl Neurobasal + B27 per well. For the mitosis assay, 10 μM BrdU was added to the culture medium. For the in vitro maturation assay, rat E14 spinal cord–derived NPCs were plated in PDL-coated six-well plates and cultured for 6 days, as described above. Cells were washed three times with calcium- and magnesium-free phosphate-buffered saline (PBS), digested in 0.25% trypsin for 5 to 10 min at 37°C, dissociated in Neurobasal media plus 10% fetal bovine serum, and then plated on myelin and PDL substrates.

Negr1 overexpression study

Rat E14 spinal cord–derived NPCs were transfected using 4D-Nucleofector with the P3 Primary Cell Kit (3 million per cuvette; Lonza). Either 3 μg of Negr1-pcDNA3 + 0.5 μg of Pmax-GFP (Lonza) or 3 μg of empty pcDNA3 backbone (31) + 0.5 μg of Pmax-GFP were used per electroporation in the 16-well Nucleocuvette Strip and plated on PDL-coated six-well plates, matured in vitro for 6 days, and replated on myelin substrates as described above.

Cell culture plate preparation and maintenance

Plates were precoated with PDL (20 μg/ml) overnight at room temperature (RT). In addition, some wells were coated with myelin or liver membranes at 10 μg/ml in PBS overnight at 4°C, or laminin (1 μg/ml; Sigma-Aldrich) for 4 hours at RT. In some experiments, 10 μM forskolin (Sigma-Aldrich), *ERK*-kinase-(*MEK*) inhibitor (10 μg/ml; PD98059), *ERK* inhibitor (12.5 μM; CAS1049738), or CSPGs (10 to 30 μg/ml; EMD Millipore) was applied to the culture medium. All cells were cultured at 37°C in 5% CO_2 for 48 hours, if not stated otherwise.

Immunocytochemistry

Cells were fixed and stained for mouse anti–βIII-tubulin (1:2000, Promega), mouse anti-Tau1 (1:200, Chemicon MAB342), rabbit anti-Map2 (1:1000, EMD Millipore AB5622), or mouse anti-BrdU, (EMD Millipore, MAB3222) as described (55). Mitosis assay was performed as described (56). Cells were imaged at 4× or 10× with ImageXpress, and neurite outgrowth was automatically quantified by MetaXpress software (Molecular Devices).

Human iPSC generation and culture

Human iPSC–derived neurons were derived and purified as described (57). Plates were precoated overnight at 37°C with poly-ornithine (40 μg/ml in water, Sigma-Aldrich), washed three times with sterile water, subsequently coated with either rat or monkey myelin (10 μg/ml in PBS) overnight at 4°C, washed three times with PBS, coated with laminin (5 μg/ml in media) for 4 hours at RT, and washed three times with media before plating of cells. Cells were cultured at 37°C in 5% CO_2 for 48 hours.

Enzyme-linked immunosorbent assay

Rat E14 NPCs were cultured as described above. Adult CNS myelin was added to the media 2 hours after plating (10 μg/ml). At 0.5, 3, 6, 24, and 48 hours posttreatment, cells were washed twice with PBS. ELISAs were performed according the manual of ERK1/2 Instant One ELISA Kit (eBioscience) and a direct cAMP ELISA kit (Enzo Life Sciences). cAMP was acetylated to increase the sensitivity of detection.

Western blot analysis

Rat E14 spinal cords were dissociated and plated in six-well tissue culture–treated plates plus laminin (1 μg/ml in PBS; Sigma-Aldrich) and/or myelin substrates at 3×10^6 cells per well. Protein samples were collected at 0.5, 3, 6, 24, and 48 hours after plating. Immunoblots were performed as previously described (25) and labeled with rabbit anti–

phospho-p44/42 MAPK (ERK1/2) (1:1000, Cell Signaling), anti- p44/42 MAPK (ERK1/2) (1:1000), anti–β-actin (1:10,000, Sigma-Aldrich), or anti-*Negr1* (1:2000, Clone 5A4.1, EMD Millipore). Blots were developed using SuperSignal West Dura ECL substrate (Thermo Fisher Scientific) and imaged using ChemiDoc MP imaging system (Bio-Rad). All blot densitometry data were quantified using Image Lab software (Bio-Rad).

RNA isolation and sequencing

Mouse E12 NPCs were cultured for 48 hours on precoated plates as described above. RNA was collected using the Absolutely RNA Nanoprep Kit (Agilent) according to the manufacturer's instructions. Total RNA integrity was examined using the Agilent Bioanalyzer 2000 (Agilent) and quantified with NanoDrop (Thermo Fisher Scientific). Total RNA (20 ng) was used to generate cDNA using Ovation RNA-Seq System V2 (NuGEN) following the manufacturer's instruction. cDNA (100 ng) was used in the library preparation using Ovation Ultralow Library Systems (NuGEN). The cDNA was fragmented to 300 base pairs (bp) using the Covaris M220 (Covaris), and then the manufacturer's instruction was followed for end repair, adaptor ligation, and library amplification. All samples were multiplexed into a single pool to avoid batch effects (58) and sequenced using an Illumina HiSeq 2500 sequencer (Illumina) across four lanes of 69-bp paired-end sequencing, corresponding to three samples per lane and yielding between 45 and 55 mil reads per sample. Alignment to the *Mus musculus* (mm10) refSeq (refFlat) reference gene annotation was performed using the STAR-spliced read aligner (v 2.3.0) (59) with default parameters. Data quality was assessed on base quality calls, nucleotide composition of sequences, insert sizes, percent of uniquely aligned reads, and transcript coverage using custom scripts (available at https://github.com/icnn/RNAseq-PIPELINE) and picard-tools-1.118 (http://broadinstitute.github.io/picard/). Read alignments were visualized using the Integrative Genomics Viewer (60). Ninety-two percent to 93% of the reads mapped uniquely to the mouse genome. Total counts of read fragments aligned to candidate gene regions were derived using the HTSeq program (www.huber.embl.de/users/anders/HTSeq/doc/overview.html) with mouse mm10 (Dec.2011) refSeq (refFlat table) as a reference and used as a basis for the quantification of gene expression. Only uniquely mapped reads were used for subsequent analyses. Differential expression analysis was conducted with R-project and the Bioconductor package edgeR (v 3.14.0) (61). Statistical significance of differential expression was determined at FDR < 10% ($q < 0.1$).

Gorilla (62) and Ingenuity Pathway Analysis software (Qiagen) were used for data analysis (complete gene list was used).

Quantitative polymerase chain reaction

Total RNA was isolated from NPC cultures using the RNeasy Mini kit (Qiagen). For cDNA synthesis, the reverse transcription reaction was performed using the PrimeScript RT Master Mix (Perfect Real Time, Clontech). Negr1 [agctggaatcttctgctgatgagc (forward) and caaaaagcactcagtactgtggcc (reverse)], Malat1 [atgtttgataccagtgctgggtgg (forward) and aaccctactgacgaatctgcttcc (reverse)], Miat [gaaaccaccagaacttctggtagc (forward) and accacctatctccagatcttctgg (reverse)], H19 [atccatcttcatggccaactctgc (forward) and gtaaatggggaaacagagtcacgg (reverse)], and Plekhb1 [tactggcaggacatacccttaacc

(forward) and atgttaacagtcgagctgagctcc (reverse)] expression was normalized to glyceraldehyde-3-phosphate dehydrogenase expression [gacttcaacagcaactcccactct (forward) and ggtttcttactccttggaggccat (reverse)].

Statistical analysis

All data are presented as the mean ± SEM if not mentioned otherwise. For quantification of axon number in white versus gray matter (Fig. 1) as well as for Western blot, ELISA, and qPCR quantification (Figs. 5, B, C, F, and G, and 7, B and D) and neurite outgrowth (Fig. 7, E and F, and figs. S3, S4, and S7), an unpaired, two-tailed Student's *t* test was used. For analysis of electron microscopy data (Fig. 2), a *Z* test was used to compute a two-tailed *P* value. For all in vitro experiments (Figs. 3 to 5, D and E, and figs. S1, S2, and S6), as well as *Negr1* RNA-seq (Fig. 7A), a one-way ANOVA with Tukey's post hoc test was applied unless noted otherwise. For RNA-seq analysis, a false detection rate of 10% (FDR $q < 0.1$) was applied (Fig. 6, A to C). In all statistical analyses, a significance criterion of $^{*}P \leq 0.05$, $^{**}P < 0.01$, $^{***}P < 0.001$, and $^{****}P < 0.0001$ was used. Individual level data for experiments with $n < 20$ can be found in table S1.

Supplementary Material

Refer to Web version on PubMed Central for supplementary material.

Funding:

This work was supported by the Veterans Administration, the NIH (grant nos. NS09881 and EB014986; to M.H.T.; and NS054734 to B.Z.), Deutsche Forschungsgemeinschaft (grant no. CRC1080; to L.M. and M.K.E.S.), The Craig H. Neilsen Foundation (to M.H.T.), the Bernard and Anne Spitzer Charitable Trust (to M.H.T.), and the Dr. Miriam and Sheldon G. Adelson Medical Research Foundation (to M.H.T.). We acknowledge the support of the NINDS (National Institute of Neurological Disorders and Stroke) Informatics Center for Neurogenetics and Neurogenomics (grant no. P30 NS062691; to G.C.).

Data and materials availability:

RNA-seq data have been deposited in the Gene Expression Omnibus repository (www.ncbi.nlm.nih.gov/geo), accession number GSE98974.

REFERENCES AND NOTES

1. Chen MS, Huber AB, van der Haar ME, Frank M, Schnell L, Spillmann AA, Christ F, Schwab ME, Nogo-A is a myelin-associated neurite outgrowth inhibitor and an antigen for monoclonal antibody IN-1. Nature403, 434–439 (2000). [PubMed: 10667796]
2. Schnell L, Schwab ME, Axonal regeneration in the rat spinal cord produced by an antibody against myelin-associated neurite growth inhibitors. Nature343, 269–272 (1990). [PubMed: 2300171]
3. GrandPré T, Nakamura F, Vartanian T, Strittmatter SM, Identification of the Nogo inhibitor of axon regeneration as a Reticulon protein. Nature403, 439–444 (2000). [PubMed: 10667797]
4. Yiu G, He Z, Glial inhibition of CNS axon regeneration. Nat. Rev. Neurosci7, 617–627 (2006). [PubMed: 16858390]
5. McKerracher L, David S, Jackson DL, Kottis V, Dunn RJ, Braun PE, Identification of myelin-associated glycoprotein as a major myelin-derived inhibitor of neurite growth. Neuron13, 805–811 (1994). [PubMed: 7524558]

6. Mukhopadhyay G, Doherty P, Walsh FS, Crocker PR, Filbin MT, A novel role for myelin-associated glycoprotein as an inhibitor of axonal regeneration. Neuron13, 757–767 (1994). [PubMed: 7522484]
7. Kottis V, Thibault P, Mikol D, Xiao Z-C, Zhang R, Dergham P, Braun PE, Oligodendrocyte-myelin glycoprotein (OMgp) is an inhibitor of neurite outgrowth. J. Neurochem82, 1566–1569 (2002). [PubMed: 12354307]
8. Wang KC, Koprivica V, Kim JA, Sivasankaran R, Guo Y, Neve RL, He Z, Oligodendrocyte-myelin glycoprotein is a Nogo receptor ligand that inhibits neurite outgrowth. Nature417, 941–944 (2002). [PubMed: 12068310]
9. Löw K, Culbertson M, Bradke F, Tessier-Lavigne M, Tuszynski MH, Netrin-1 is a novel myelin-associated inhibitor to axon growth. J. Neurosci28, 1099–1108 (2008). [PubMed: 18234888]
10. Benson MD, Romero MI, Lush ME, Lu QR, Henkemeyer M, Parada LF, Ephrin-B3 is a myelin-based inhibitor of neurite outgrowth. Proc. Natl. Acad. Sci. U.S.A102, 10694–10699 (2005). [PubMed: 16020529]
11. Lee JK, Geoffroy CG, Chan AF, Tolentino KE, Crawford MJ, Leal MA, Kang B, Zheng B, Assessing spinal axon regeneration and sprouting in Nogo-, MAG-, and OMgp-deficient mice. Neuron66, 663–670 (2010). [PubMed: 20547125]
12. GrandPré T, Li S, Strittmatter SM, Nogo-66 receptor antagonist peptide promotes axonal regeneration. Nature417, 547–551 (2002). [PubMed: 12037567]
13. Kadoya K, Lu P, Nguyen K, Lee-Kubli C, Kumamaru H, Yao L, Knackert J, Poplawski G, Dulin JN, Strobl H, Takashima Y, Biane J, Conner J, Zhang S-C, Tuszynski MH, Spinal cord reconstitution with homologous neural grafts enables robust corticospinal regeneration. Nat. Med22, 479–487 (2016). [PubMed: 27019328]
14. Lu P, Wang Y, Graham L, McHale K, Gao M, Wu D, Brock J, Blesch A, Rosenzweig ES, Havton LA, Zheng B, Conner JM, Marsala M, Tuszynski MH, Long-distance growth and connectivity of neural stem cells after severe spinal cord injury. Cell150, 1264–1273 (2012). [PubMed: 22980985]
15. Lu P, Woodruff G, Wang Y, Graham L, Hunt M, Wu D, Boehle E, Ahmad R, Poplawski G, Brock J, Goldstein LSB, Tuszynski MH, Long-distance axonal growth from human induced pluripotent stem cells after spinal cord injury. Neuron83, 789–796 (2014). [PubMed: 25123310]
16. Rosenzweig ES, Brock JH, Lu P, Kumamaru H, Salegio EA, Kadoya K, Weber JL, Liang JJ, Moseanko R, Hawbecker S, Huie JR, Havton LA, Nout-Lomas YS, Ferguson AR, Beattie MS, Bresnahan JC, Tuszynski MH, Restorative effects of human neural stem cell grafts on the primate spinal cord. Nat. Med24, 484–490 (2018). [PubMed: 29480894]
17. Lu P, Blesch A, Graham L, Wang Y, Samara R, Banos K, Haringer V, Havton L, Weishaupt N, Bennett D, Fouad K, Tuszynski MH, Motor axonal regeneration after partial and complete spinal cord transection. J. Neurosci32, 8208–8218 (2012). [PubMed: 22699902]
18. Turnley AM, Bartlett PF, MAG and MOG enhance neurite outgrowth of embryonic mouse spinal cord neurons. Neuroreport9, 1987–1990 (1998). [PubMed: 9674579]
19. Shewan D, Berry M, Cohen J, Extensive regeneration in vitro by early embryonic neurons on immature and adult CNS tissue. J. Neurosci15, 2057–2062 (1995). [PubMed: 7891152]
20. Qiu J, Cai D, Dai H, McAtee M, Hoffman PN, Bregman BS, Filbin MT, Spinal axon regeneration induced by elevation of cyclic AMP. Neuron34, 895–903 (2002). [PubMed: 12086638]
21. Bradbury EJ, Moon LDF, Popat RJ, King VR, Bennett GS, Patel PN, Fawcett JW, McMahon SB, Chondroitinase ABC promotes functional recovery after spinal cord injury. Nature416, 636–640 (2002). [PubMed: 11948352]
22. Silver J, Miller JH, Regeneration beyond the glial scar. Nat. Rev. Neurosci5, 146–156 (2004). [PubMed: 14735117]
23. Chierzi S, Ratto GM, Verma P, Fawcett JW, The ability of axons to regenerate their growth cones depends on axonal type and age, and is regulated by calcium, cAMP and ERK. Eur. J. Neurosci21, 2051–2062 (2005). [PubMed: 15869501]
24. Puttagunta R, Tedeschi A, Sória MG, Hervera A, Lindner R, Rathore KI, Gaub P, Joshi Y, Nguyen T, Schmandke A, Laskowski CJ, Boutillier A-L, Bradke F, Di Giovanni S, PCAF-dependent epigenetic changes promote axonal regeneration in the central nervous system. Nat. Commun5, 3527 (2014). [PubMed: 24686445]

25. Perron JC, Bixby JL, Distinct neurite outgrowth signaling pathways converge on ERK activation. Mol. Cell. Neurosci13, 362–378 (1999). [PubMed: 10356298]
26. Cai D, Qiu J, Cao Z, McAtee M, Bregman BS, Filbin MT, Neuronal cyclic AMP controls the developmental loss in ability of axons to regenerate. J. Neurosci21, 4731–4739 (2001). [PubMed: 11425900]
27. Ming G-L, Song H-J, Berninger B, Holt CE, Tessier-Lavigne M, M.-m. Poo, cAMP-dependent growth cone guidance by netrin-1. Neuron19, 1225–1235 (1997). [PubMed: 9427246]
28. Cai D, Shen Y, De Bellard M, Tang S, Filbin MT, Prior exposure to neurotrophins blocks inhibition of axonal regeneration by MAG and myelin via a cAMP-dependent mechanism. Neuron22, 89–101 (1999). [PubMed: 10027292]
29. Schäfer M, Bräuer AU, Savaskan NE, Rathjen FG, Brümmendorf T, Neurotractin/kilon promotes neurite outgrowth and is expressed on reactive astrocytes after entorhinal cortex lesion. Mol. Cell. Neurosci29, 580–590 (2005). [PubMed: 15946856]
30. Pischedda F, Piccoli G, The IgLON family member Negr1 promotes neuronal arborization acting as soluble factor via FGFR2. Front. Mol. Neurosci8, 89 (2016). [PubMed: 26793057]
31. Lee AWS, Hengstler H, Schwald K, Berriel-Diaz M, Loreth D, Kirsch M, Kretz O, Haas CA, de Angelis MH, Herzig S, Brümmendorf T, Klingenspor M, Rathjen FG, Rozman J, Nicholson G, Cox RD, Schäfer MKE, Functional inactivation of the genome-wide association study obesity gene neuronal growth regulator 1 in mice causes a body mass phenotype. PLOS ONE7, e41537 (2012). [PubMed: 22844493]
32. Zörner B, Schwab ME, Anti-Nogo on the go: From animal models to a clinical trial. Ann. N. Y. Acad. Sci1198, (Suppl 1) E22–E34 (2010). [PubMed: 20590535]
33. Dulin JN, Adler AF, Kumamaru H, Poplawski GHD, Lee-Kubli C, Strobl H, Gibbs D, Kadoya K, Fawcett JW, Lu P, Tuszynski MH, Injured adult motor and sensory axons regenerate into appropriate organotypic domains of neural progenitor grafts. Nat. Commun9, 84 (2018). [PubMed: 29311559]
34. Richardson WDD, Pringle NP, Yu W-P, Hall AC, Origins of spinal cord oligodendrocytes: Possible developmental and evolutionary relationships with motor neurons. Dev. Neurosci19, 58–68 (1997). [PubMed: 9078434]
35. Davies SJ, Field PM, Raisman G, Long interfascicular axon growth from embryonic neurons transplanted into adult myelinated tracts. J. Neurosci14, 1596–1612 (1994). [PubMed: 8126557]
36. Fujii M, Non-specific characteristics of intracerebral fiber elongation from the olfactory bulb transplanted into the young adult host neocortex or hippocampal formation, demonstrated immunohistochemically by the mouse Thy-1 allelic system. Neurosci. Res9, 285–291 (1991). [PubMed: 1674127]
37. Strömberg I, Bygdeman M, Almqvist P, Target-specific outgrowth from human mesencephalic tissue grafted to cortex or ventricle of immunosuppressed rats. J. Comp. Neurol315, 445–456 (1992). [PubMed: 1348513]
38. Tønder N, Sørensen T, Zimmer J, Grafting of fetal CA3 neurons to excitotoxic, axon-sparing lesions of the hippocampal CA3 area in adult rats. Prog. Brain Res83, 391–409 (1990). [PubMed: 2392568]
39. Wictorin K, Brundin P, Sauer H, Lindvall O, Björklund A, Long distance directed axonal growth from human dopaminergic mesencephalic neuroblasts implanted along the nigrostriatal pathway in 6-hydroxydopamine lesioned adult rats. J. Comp. Neurol323, 475–494 (1992). [PubMed: 1358925]
40. Wictorin K, Lagenaur CF, Lund RD, Björklund A, Efferent projections to the host brain from intrastriatal striatal mouse-to-rat grafts: time course and tissue-type specificity as revealed by a mouse specific neuronal marker. Eur. J. Neurosci3, 86–101 (1991). [PubMed: 12106272]
41. Davies SJA, Fitch MT, Memberg SP, Hall AK, Raisman G, Silver J, Regeneration of adult axons in white matter tracts of the central nervous system. Nature390, 680–683 (1997). [PubMed: 9414159]
42. Davies SJA, Goucher DR, Doller C, Silver J, Robust regeneration of adult sensory axons in degenerating white matter of the adult rat spinal cord. J. Neurosci19, 5810–5822 (1999). [PubMed: 10407022]

43. Jones LL, Yamaguchi Y, Stallcup WB, Tuszynski MH, NG2 is a major chondroitin sulfate proteoglycan produced after spinal cord injury and is expressed by macrophages and oligodendrocyte progenitors. J. Neurosci22, 2792–2803 (2002). [PubMed: 11923444]
44. Lemons ML, Howland DR, Anderson DK, Chondroitin sulfate proteoglycan immunoreactivity increases following spinal cord injury and transplantation. Exp. Neurol160, 51–65 (1999). [PubMed: 10630190]
45. Massey JM, Amps J, Viapiano MS, Matthews RT, Wagoner MR, Whitaker CM, Alilain W, Yonkof AL, Khalyfa A, Cooper NGF, Silver J, Onifer SM, Increased chondroitin sulfate proteoglycan expression in denervated brainstem targets following spinal cord injury creates a barrier to axonal regeneration overcome by chondroitinase ABC and neurotrophin-3. Exp. Neurol209, 426–445 (2008). [PubMed: 17540369]
46. Andrews EM, Richards RJ, Yin FQ, Viapiano MS, Jakeman LB, Alterations in chondroitin sulfate proteoglycan expression occur both at and far from the site of spinal contusion injury. Exp. Neurol235, 174–187 (2012). [PubMed: 21952042]
47. Busch SA, Horn KP, Cuascut FX, Hawthorne AL, Bai L, Miller RH, Silver J, Adult NG2+ cells are permissive to neurite outgrowth and stabilize sensory axons during macrophage-induced axonal dieback after spinal cord injury. J. Neurosci30, 255–265 (2010). [PubMed: 20053907]
48. Grumet M, Milev P, Sakurai T, Karthikeyan L, Bourdon M, Margolis RK, Margolis RU, Interactions with tenascin and differential effects on cell adhesion of neurocan and phosphacan, two major chondroitin sulfate proteoglycans of nervous tissue. J. Biol. Chem269, 12142–12146 (1994). [PubMed: 7512960]
49. Margolis RK, Rauch U, Maurel P, Margolis RU, Neurocan and phosphacan: Two major nervous tissue-specific chondroitin sulfate proteoglycans. Perspect. Dev. Neurobiol3, 273–290 (1996). [PubMed: 9117260]
50. Yi J-H, Katagiri Y, Susarla B, Figge D, Symes AJ, Geller HM, Alterations in sulfated chondroitin glycosaminoglycans following controlled cortical impact injury in mice. J. Comp. Neurol520, 3295–3313 (2012). [PubMed: 22628090]
51. Marg A, Sirim P, Spaltmann F, Plagge A, Kauselmann G, Buck F, Rathjen FG, Brümmendorf T, Neurotractin, a novel neurite outgrowth-promoting Ig-like protein that interacts with CEPU-1 and LAMP. J. Cell Biol145, 865–876 (1999). [PubMed: 10330412]
52. Kaplan A, Kent CB, Charron F, Fournier AE, Switching responses: Spatial and temporal regulators of axon guidance. Mol. Neurobiol49, 1077–1086 (2014). [PubMed: 24271658]
53. Hunt M, Lu P, Tuszynski MH, Myelination of axons emerging from neural progenitor grafts after spinal cord injury. Exp. Neurol296, 69–73 (2017). [PubMed: 28698030]
54. Larocca JN, Norton WT, Isolation of myelin. Curr. Protoc. Cell BiolChapter 3, 3.25.1–3.25.19 (2007). [PubMed: 18228504]
55. McCall J, Nicholson L, Weidner N, Blesch A, Optimization of adult sensory neuron electroporation to study mechanisms of neurite growth. Front. Mol. Neurosci5, 11 (2012). [PubMed: 22347167]
56. Mühlmann-Díaz MC, Dullea RG, Bedford JS, Application of 5-bromo-2′deoxyuridine as a label for in situ hybridization in chromosome microdissection and painting, and 3′ OH DNA end labeling for apoptosis. Biotechniques21, 82–86 (1996). [PubMed: 8816240]
57. Israel MA, Yuan SH, Bardy C, Reyna SM, Mu Y, Herrera C, Hefferan MP, Van Gorp S, Nazor KL, Boscolo FS, Carson CT, Laurent LC, Marsala M, Gage FH, Remes AM, Koo EH, Goldstein LS, Probing sporadic and familial Alzheimer's disease using induced pluripotent stem cells. Nature482, 216–220 (2012). [PubMed: 22278060]
58. Auer PL, Doerge RW, Statistical design and analysis of RNA sequencing data. Genetics185, 405–416 (2010). [PubMed: 20439781]
59. Dobin A, Davis CA, Schlesinger F, Drenkow J, Zaleski C, Jha S, Batut P, Chaisson M, Gingeras TR, STAR: Ultrafast universal RNA-seq aligner. Bioinformatics29, 15–21 (2013). [PubMed: 23104886]
60. Robinson JT, Thorvaldsdóttir H, Winckler W, Guttman M, Lander ES, Getz G, Mesirov JP, Integrative genomics viewer. Nat. Biotechnol29, 24–26 (2011). [PubMed: 21221095]

61. Robinson MD, McCarthy DJ, Smyth GK, edgeR: A Bioconductor package for differential expression analysis of digital gene expression data. Bioinformatics26, 139–140 (2010). [PubMed: 19910308]

62. Eden E, Navon R, Steinfeld I, Lipson D, Yakhini Z, *GOrilla*: A tool for discovery and visualization of enriched GO terms in ranked gene lists. BMC Bioinformatics10, 48 (2009). [PubMed: 19192299]

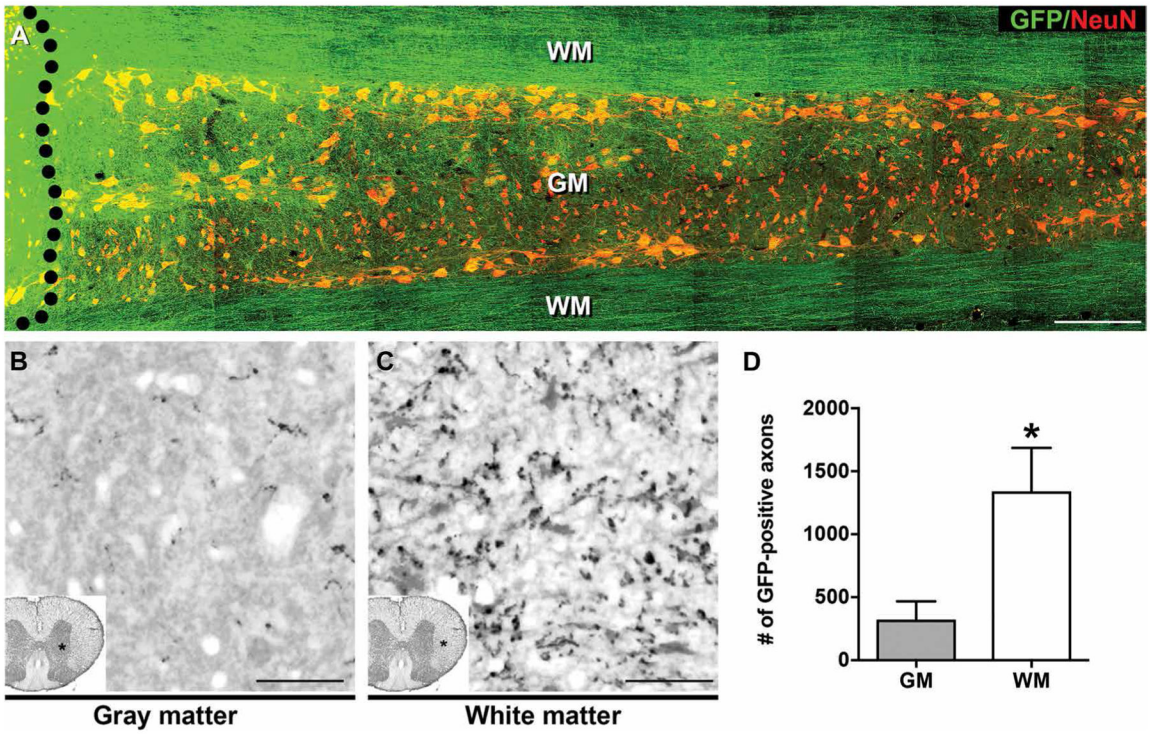

Fig. 1. Rat NPCs extend greater numbers of axons into spinal cord white matter than gray matter.

(**A**) GFP-expressing E14 rat spinal cord–derived NPCs were grafted into sites of C5 spinal cord hemisection lesions (black dotted line indicates graft boundary) 2 weeks after injury. One month after grafting, horizontal sections of spinal cord were immunolabeled for GFP (green) and the neuronal marker NeuN (red). Immunolabeling indicated that rat NPCs extended their axons through spinal cord host white matter (WM) and gray matter (GM). Greater numbers of axons appeared to extend through WM than GM. The rostral section of spinal cord is on the left, and the caudal section is on the right. (**B** and **C**) GFP immunolabeling of rat NPC graft–derived axons in transverse sections of rat spinal cord demonstrated larger numbers of axons extending into caudal host spinal cord white matter, three spinal segments below the graft site. (**D**) Quantification of data in (B) and (C). Mean ± SEM (*$P < 0.05$, paired, two-tailed t test; $n = 4$ rats). Scale bars, 500 μm (A), 25 μm (B and C).

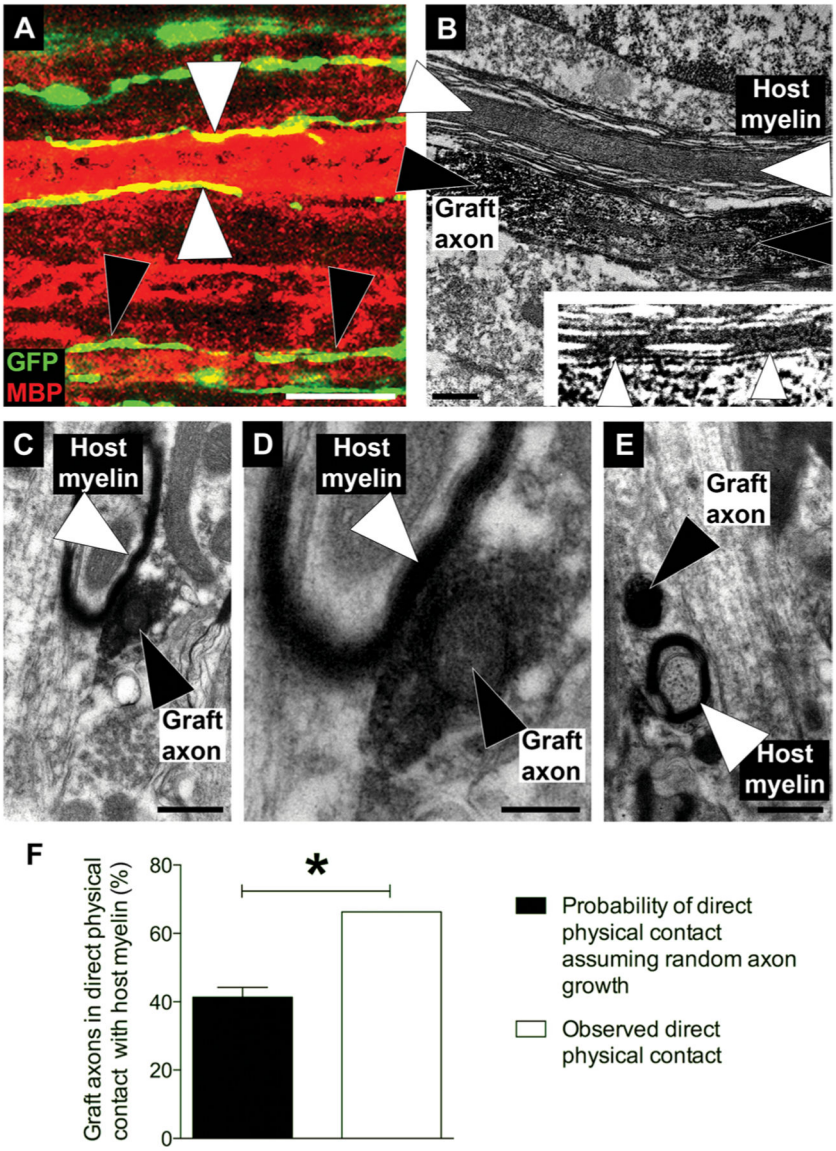

Fig. 2. Human NSC–derived and rodent NPC–derived neurons preferentially associate with host myelin.

(**A**) GFP-labeled human induced pluripotent stem cells (iPSC)–derived NSCs (green) were grafted into sites of C5 hemisection lesions in immunodeficient rats. GFP-expressing graft-derived axons (green/yellow) are shown extending along myelin basic protein (MBP)–immunoreactive intact rat host myelin (red; white arrowheads) and degenerating rat host myelin (black arrowheads). The section shown was taken from six spinal cord segments (T3) below the lesion/graft site. (**B**) Electron micrograph showing apposition of a rat NPC graft–derived axon from an E14 rat spinal cord–derived NPC graft (black arrowhead) to rat host myelin (white arrowheads). Section was taken two spinal cord segments below a graft placed at a C5 hemisection lesion site. The graft axons are immunogold-labeled for GFP. (Inset) Higher magnification inset showing rat NPC graft–derived axon directly in contact with rat host myelin. (**C** to **E**) Transverse sections taken two spinal cord segments caudal to the graft site, showing association of GFP-immunoreactive rat NPC graft–derived

axons with rat host myelin. (C) GFP-immunoreactive rat NPC graft–derived axon in contact with rat host myelin. (D) Higher magnification image of (C). (E) GFP-labeled rat NPC graft–derived axon not in direct contact with rat host myelin (**F**) Percentage of GFP-positive graft-derived axons in direct physical contact with host myelin compared to the probability of direct physical contact assuming random axon growth. Sixty-five percent of graft-derived axons directly contacted rat host myelin. Mean ± SEM (*$P < 0.05$, Z test; $n = 105$ axons). Scale bars, 10 μm (A), 0.5 μm (B, C, and E), and 0.2 μm (D).

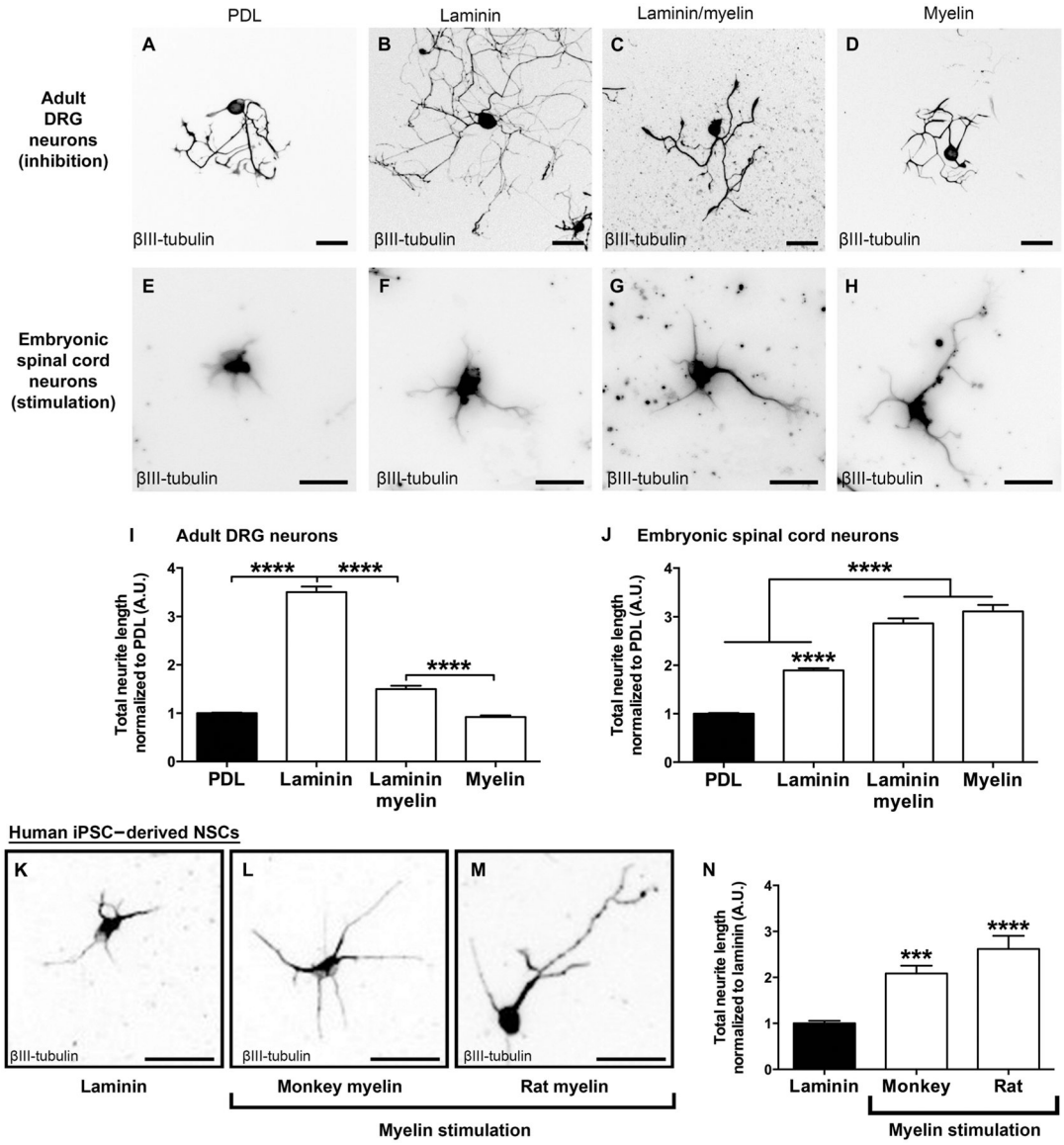

Fig. 3. Human NSC-derived and rat NPC–derived axon growth is stimulated by myelin in vitro.

(**A** to **D**) Adult rat DRG neurons plated on laminin exhibited increased growth, which was inhibited by myelin as expected. This inhibition is quantified in (**I**) (****$P < 0.0001$, one-way ANOVA with post hoc Tukey's test; $n = 3$ rats; $n = 4$ wells per rat). (**E** to **H**) E14 rat spinal cord–derived NPCs exhibited stimulation of neurite growth on myelin, but not laminin. This growth stimulation is quantified in (**J**) (****$P < 0.0001$, one-way ANOVA with post hoc Tukey's test; $n = 9$ rat embryos, $n = 2$ to 3 wells per embryo). Values are normalized to the poly-D-lysine (PDL) substrate for each individual experiment. (**K** to **M**) Neurite outgrowth from human iPSC–derived NSCs was stimulated on myelin derived from either monkey or rat spinal cord. A βIII-tubulin label was used to identify axons and is quantified in (**N**). Values are normalized to the laminin substrate (a required substrate for culturing iPSC-derived NSCs) for each individual experiment (****$P < 0.0001$, one-way ANOVA, with ***$P < 0.001$, ****$P < 0.0001$ post hoc Tukey's test; $n = 3$ individual

experiments, n = 6 to 10 wells per experiment). Mean ± SEM. Scale bars, 100 μm (A to D), 30 μm (E to H), and 20 μm (K to M). A.U., arbitrary units.

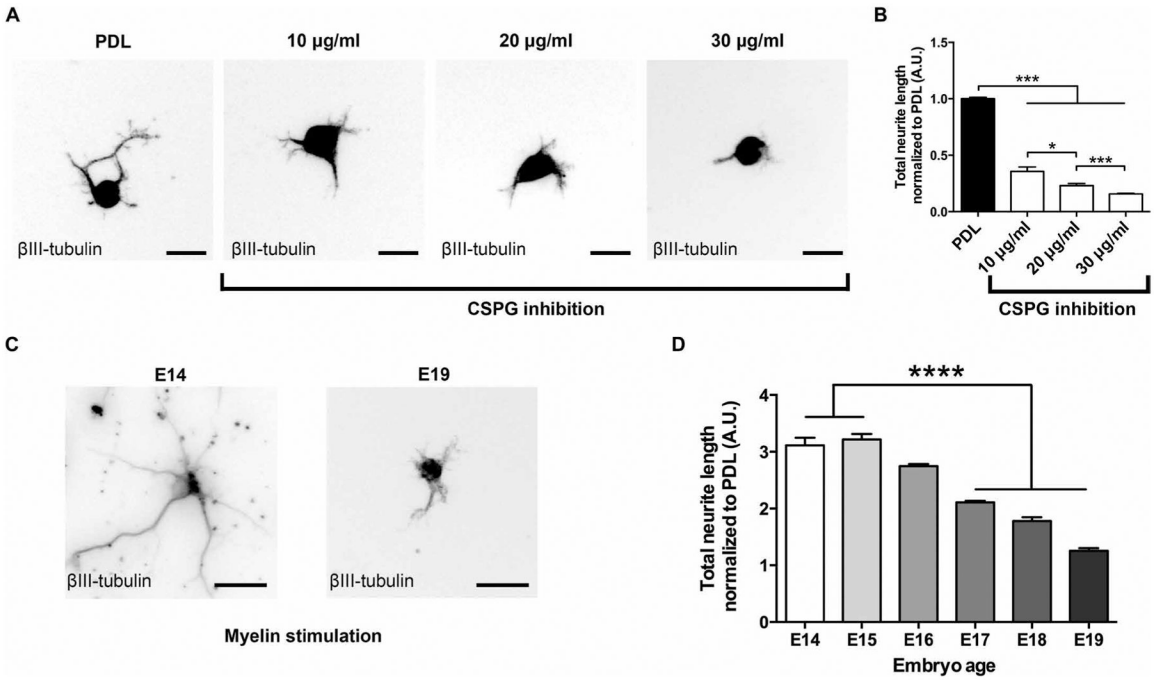

Fig. 4. Rat NPCs are inhibited by CSPGs.

(**A** and **B**) Neurite outgrowth from E14 rat spinal cord–derived NPCs was inhibited by CSPG in a dose-dependent manner (***$P < 0.001$, one-way ANOVA, with *$P < 0.05$, ***$P < 0.001$ post hoc Tukey's test; $n = 3$ rat spinal cords, $n = 2$ wells per spinal cord). (**C** and **D**) Myelin-dependent neurite outgrowth from rat NPCs derived from rat embryos at different developmental stages was developmentally regulated and declined steadily from E14 to E19 (****$P < 0.0001$, one-way ANOVA with post hoc Tukey's test; $n = 3$ embryos per time point, $n = 4$ wells per embryo). Values are normalized to the PDL substrate for each individual experiment. Mean ± SEM. Scale bars, 20 µm (A), 30 µm (C).

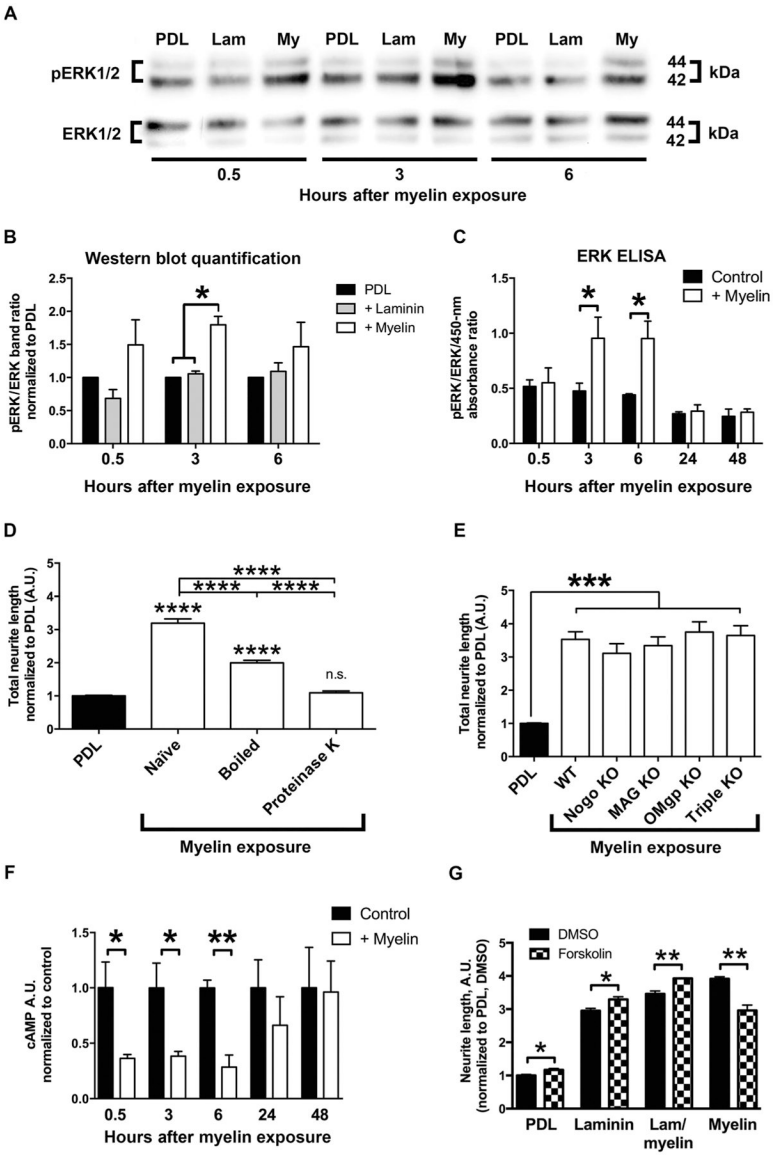

Fig. 5. Myelin activates pERK and reduces cAMP in rat NPCs.

(**A** to **C**) Extracellular signal–regulated kinase (ERK) is activated in cultures of E14 rat spinal cord–derived NPCs grown on PDL, laminin (Lam), or myelin substrates as indicated by (A and B) Western blot ($n = 3$) and (C) ELISA (*$P < 0.05$, two-tailed t test; $n = 2$ ELISAs with $n = 3$ to 4 wells per condition). (**D**) Neurite-myelin interactions are mediated by soluble protein ligands; boiling or proteinase K digestion significantly attenuated myelin-mediated activation of neurite outgrowth from E14 rat spinal cord–derived NPCs ($n = 3$ embryos, $n = 3$ to 4 wells per embryo). (**E**) Neurite outgrowth from mouse E12 spinal cord–derived NPCs is not inhibited in the presence of myelin isolated from either *Nogo*, *MAG*, or *OMgp* knockout (KO) mice, or the triple knockout compared to wild-type (WT) myelin ($n = 3$ to 4 embryos, $n = 2$ to 3 wells per embryo; ****$P < 0.0001$, one-way ANOVA, with *$P < 0.05$, ***$P < 0.001$, ****$P < 0.0001$ post hoc Tukey's test; n.s., not significant). (**F**) cAMP is reduced upon exposure of E14 rat spinal cord–derived NPCs to myelin as

shown by ELISA (*$P \leq 0.05$, **$P < 0.01$, two-tailed *t* test; $n = 2$ ELISAs, $n = 3$ wells per condition). (**G**) Forskolin (1 mM) administration to increase neuronal cAMP in E14 rat spinal cord–derived NPC cultures resulted in slightly higher neurite outgrowth on laminin, but significantly reduced neurite outgrowth on myelin after 24 hours in vitro (*$P < 0.05$, **$P < 0.01$, two-tailed *t* test; $n = 3$ embryos, $n = 2$ to 3 wells per embryo). All values are normalized to the PDL or PDL dimethyl sulfoxide (DMSO) condition for each individual experiment. Mean ± SEM.

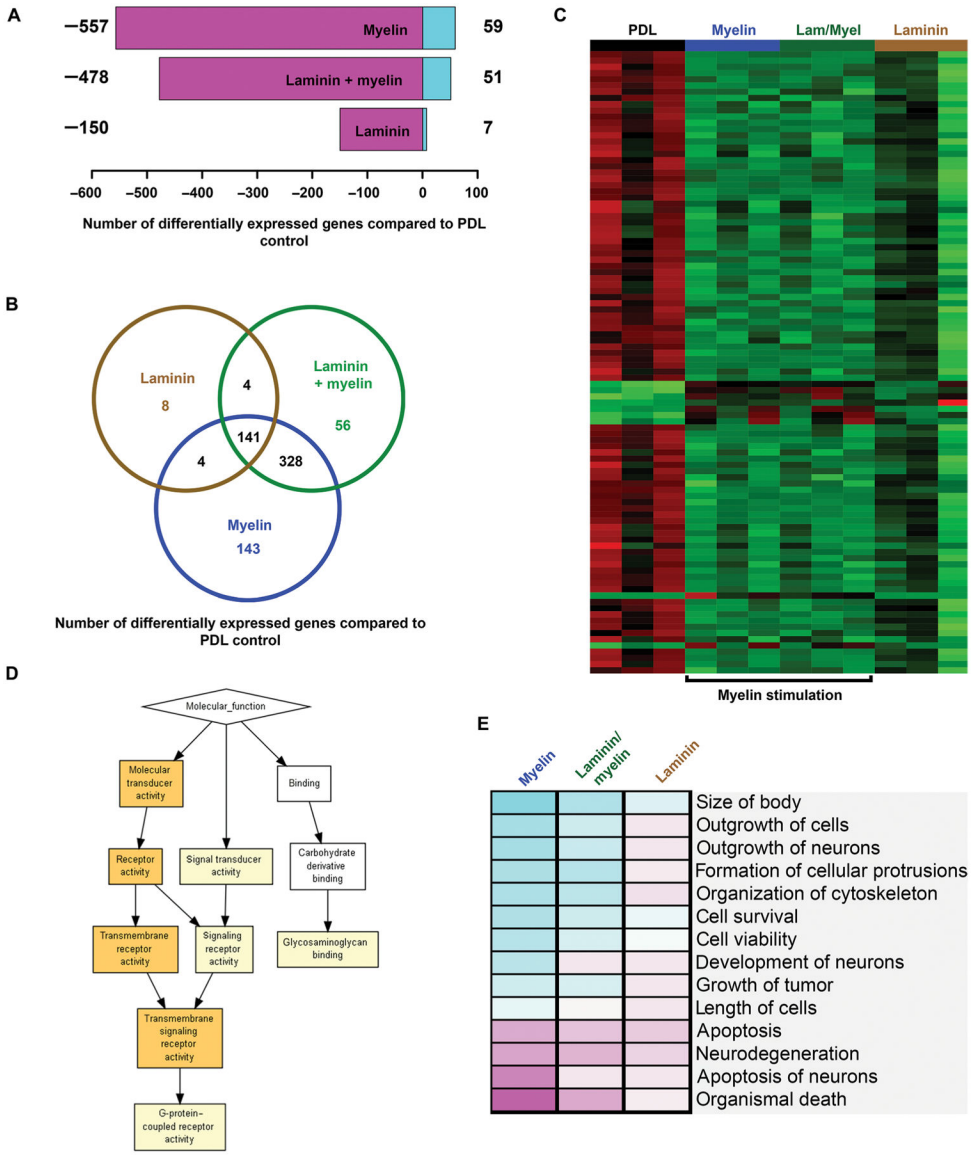

Fig. 6. RNA-seq of rat NPCs exposed to myelin.

(**A**) Shown is the number of differentially expressed transcripts revealed by RNA-seq in mouse E12 spinal cord–derived NPCs cultured on myelin, laminin/myelin, or laminin substrates compared to PDL control substrate [false discovery rate (FDR) < 0.1, $n = 3$ replicates per condition]. Down-regulated transcripts are shown in magenta and up-regulated transcripts in turquoise. (**B**) Venn diagram showing uniquely regulated and overlapping transcripts for mouse E12 spinal cord–derived NPCs cultured on myelin substrate (blue), laminin/myelin substrate (green), or laminin substrate alone (brown) compared to PDL control substrate (FDR < 0.1). (**C**) Heatmap of the 100 most differentially regulated transcripts (FDR < 0.1). Increased expression is shown in red, and reduced expression is shown in green. Transcripts and experimental groups are arranged by hierarchical clustering. Note that experimental groups that contain myelin cluster together. (**D**) Gene ontology (GO) enrichment analysis of up-regulated transcripts upon myelin stimulation compared to PDL

substrate via GOrilla (complete gene list enrichment *P* value: yellow box = 10^{-3} to 10^{-5}, orange box = 10^{-5} to 10^{-7}). (**E**) Cellular functions of proteins encoded by genes in the gene expression data set assigned using the Ingenuity Pathway analysis software (complete gene list). Predicted activation of cellular function is indicated in turquoise and predicted inhibition in magenta (saturation of color correlates with confidence of prediction).

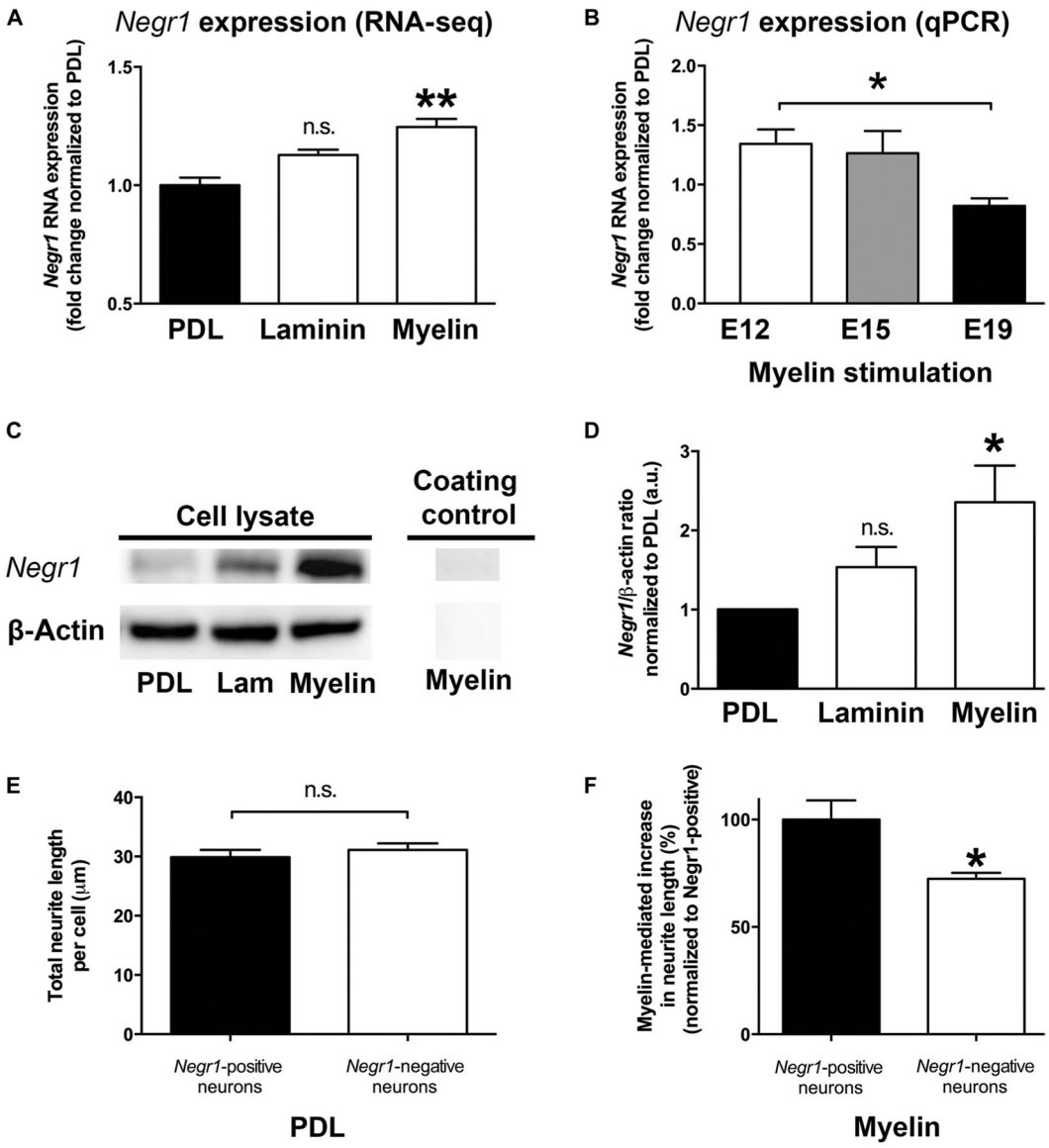

Fig. 7. Negr1 mediates the effects of myelin on mouse NPC neurite outgrowth.

(**A**) *Negr1* mRNA expression in mouse E12 spinal cord–derived NPCs significantly increased on a myelin substrate compared to a laminin or PDL substrate as shown by RNA-seq (one-way ANOVA with $^{**}P < 0.01$ post hoc Tukey's test; $n = 3$). (**B**) qPCR shows reduced *Negr1* mRNA expression in mouse E12 spinal cord–derived NPCs grown on a myelin substrate as a function of embryonic age ($^{*}P < 0.05$ two-tailed t test; $n = 3$ individual experiments). (**C**) Western blot showing increases in *Negr1* protein in mouse E12 spinal cord–derived NPCs after plating on myelin, but not laminin (Lam) or PDL. β-Actin is the loading control. (**D**) Quantification of Western blot shown in (C) ($^{*}P < 0.05$ two-tailed t test; $n = 5$ individual experiments). (**E**) E12 spinal cord–derived NPCs from *Negr1*-deficient mice displayed no change in baseline neurite growth observed on a PDL substrate. (**F**) A 25% reduction in myelin-mediated neurite outgrowth from E12 spinal cord–derived NPCs

from *Negr1*-deficient mice was observed (*$P < 0.05$ two-tailed *t* test; $n = 5$ embryos per genotype, $n = 4$ wells per embryo. Mean ± SEM for all panels.